REVISTA MATÉRIA V.26 N.04

ISSN 1517-7076 articles e13116, 2021

ABX_3 inorganic halide perovskites for solar cells: chemical and crystal structure stability

Cristian Moisés Díaz-Acosta[1], Antonia Martínez-Luévanos[1], Sofía Estrada-Flores[1], Lucia Fabiola Cano-Salazar[2], Elsa Nadia Aguilera-González[1], María Cristina Ibarra-Alonso[3]

[1] Universidad Autónoma de Coahuila. School of Chemical Sciences, Department of Advanced Ceramic Materials and Energy, Blvd. V. Carranza s/n, 25280. Saltillo, Coahuila, Mexico.
[2] Universidad Autónoma de Coahuila. School of Chemical Sciences. Department of Advanced Materials, Blvd. V. Carranza s/n, 25280. Saltillo, Coahuila, Mexico.
[3] CONACYT-Universidad Autónoma de Coahuila, School of Chemical Sciences, Blvd. V. Carranza s/n, 25280. Saltillo, Coahuila, Mexico.
e-mail: cristian.diaz@uadec.edu.mx, aml15902@uadec.edu.mx, s_estrada@uadec.edu.mx, elsaaguilera@uadec.edu.mx, lucia.cano@uadec.edu.mx, ibarra.cristina@uadec.edu.mx

RESUMEN

La energía solar es una de las tecnologías más prometedoras y desarrolladas de los últimos años, debido a su alta eficiencia y bajo costo. En este sentido, las celdas solares de tipo perovskita han sido el foco de atención de la comunidad científica mundial. El objetivo principal de este trabajo es presentar un análisis de diversas investigaciones reportadas sobre la síntesis y desarrollo de películas fotoactivas de perovskita ABX_3 para celdas solares, con énfasis en el efecto que la temperatura y la humedad tienen sobre la estabilidad de su estructura química y cristalina de la perovskita inorgánica ABX_3. En cuanto a la estructura de las celdas fotovoltaicas basadas en perovskitas inorgánicas tipo ABX_3, se presenta un análisis sobre los materiales de los que están conformadas y sobre la mejora de la eficiencia (PCS), factor de llenado (FF), densidad de corriente a corto circuito (J_{sc}) y del voltaje a circuito abierto (V_{oc}) de estos dispositivos. A manera de conclusión, se presenta una relación de los métodos, variables de síntesis y tipo de perovskita inorgánica utilizados para el desarrollo de dispositivos fotovoltaicos con las mejores eficiencias; también se resaltan las tendencias hacia las que se dirige esta área importante de la ciencia.

Palabras clave: Perovskitas inorgánicas, propiedades optoelectrónicas, estabilidad química, estructura cristalina, métodos de obtención.

ABSTRACT

Solar energy is one of the most promising and developed technologies in recent years, due to its high efficiency and low cost. Perovskite-type solar cells have been the focus of attention by the world scientific community. The main objective of this article is to present an (PSCs) analysis of the various investigations reported on the development of ABX_3 inorganic halide perovskite-based solar cells, with emphasis in the effect that temperature and humidity have on their chemical and crystal structure stability. The main methods that are used to obtain ABX_3 inorganic halide perovskites are also presented and analyzed. An analysis about the structure of these photovoltaic cells and how to improve their efficiency (PCS), fill factor (FF), short circuit current density (J_{sc}) and open circuit voltage (V_{oc}) of these devices is presented. As a conclusion, a relationship of the methods, synthesis variables, and type of inorganic halide perovskite used for the development of devices with the best efficiencies is presented; the trends towards which this area of science is heading are also highlighted.

Keywords: Inorganic perovskites, opto-electronics properties, chemical stability, crystal structure, obtention methods.

1. INTRODUCTION

Solar energy is one of the most promising alternatives to handle world energy demand, for which it is necessary to develop new materials and devices, such as solar cells, that allow it to be used more efficiently. The

Corresponding author: Antonia Martínez-Luévanos Received on: 08/03/2021 Accepted on: 02/08/2021

materials used for the manufacture of photovoltaic cells are those that convert photons into electrons through the photoelectric effect. This is why the search for materials that have the ability to absorbing light for application in photovoltaic devices has focused on materials ranging from metallic oxides, such as silicon, organic dyes, semiconductor polymers, as well as other chemical structures capable of performing this function, such as metal halide perovskites, which have a small band gap, charge mobility, low excitonic energy, long diffusion lengths, and high carrier mobility. Those materials are the basis for different generations of solar cells, the latter being used in perovskite solar cells (PSCs) [1-7].

The work describing the use of perovskites as an absorbent layer was published in 2009 when Miyasaka et al., used lead halides and methyl ammonium (MA) perovskites in a Grätzel-type cell, which use liquid electrolytes. Although the efficiency of these cells was only 3.8%, they paved the way for the development of current PSCs, which have reached efficiencies greater than 22%, for which the liquid electrolyte was changed for semiconductors carrying solid hollows [8, 9]. Nowadays, the PSCs are cells n-i-p type where (n) is an electron transporting layer (ETL) typically TiO_2, (i) is the perovskite totally inorganic or with an inorganic cation and (p) is an organic or inorganic hole transporting layer (HTL) [10-12]. Although the efficiency of these devices has reached levels that makes them a real alternative for their application and use in large-scale clean energy generation, they still present points of improvement, such as the chemical and structural stability of perovskite. As mentioned before, the first perovskite used for this purpose consisted of methyl ammonium and lead halides, particularly $CH_3NH_2PbI_3$ (MAPI) and $CH_5N_2PbBr_3$ (FAPBr), which are still being used and are the ones with the highest efficiency. However, these structures have a low stability against to factors such as the presence of humidity and the presence of oxygen, in addition to being unstable at temperatures above 85 °C, low formation energy, etc., making it difficult to apply in environmental conditions. Due to the above, research is continuing on the synthesis of perovskites and the development of solar cells based on perovsquites that do not present these deficiencies [10, 13-16]. Inorganic perovskites appeared as a possible solution to the deficiencies on chemical stability presented by organic/inorganic perovskites, since temperature affects the crystal structure but does not degrade its components, which is vital for devices that will be exposed to solar radiation. Inorganic perovskite solar cells have lower efficiencies than organic/inorganic perovskite-based cells [17, 18].

The most used cation to replace another cation in the structure of the organic perovskite $MABX_3$ has been the Cs, radically increasing stability. Inorganic perovskites are not so hygroscopic and withstand high temperatures unlike their organic / inorganic counterpart, however, far from being presented as the definitive solution for application in photoconversion processes, they still need to be adapted, since they present different crystallographic arrangements and not all of them are photoactive [19-22].

The main inorganic perovskites currently used are $CsPbI_3$, $CsPbBr_3$ and $CsPbI_yBr_{3-y}$. The first one has a band gap that is very close to 1.73 eV, this structure presents a black coloration in its cubic phase that turns yellow once it decays to its orthorhombic form, which is inactive and more stable at room temperature, which is thermodynamically favorable, even when it is kept free of moisture and invariably occurs within a few days at most [23-26]. The perovskite $CsPbBr_3$ has a gap band width of nearly to 2.3 eV, in its cubic phase, this is the most stable of the inorganic perovskites at room temperature. It has been reported that photovoltaic devices manufactured with this perovskites exceed the 2000 hours of use, nevertheless, in comparison with $CsPbI_3$, it has lower photoconversion efficiency [27-31], that is why the inclusion of Br^- and I^- in the same perovskite ABX_3 ($X=Br_{3-y}$, I_y) lead to obtain a structure that presents better efficiencies than those that only have Br^- and better stability than I^- perovskites [32-34]. The inclusion in the crystalline network of cations such as K, Zn, Bi, has also been explored to modify the size of the crystallite and favor its stability under environmental conditions. Some researchers have chosen to replace the Pb of perovskite due to the toxicity of this element. The lead-free $CsSnX_3$ perovskite has very low percentages of photoconversion efficiency [35-40]. This work aims to provide a current perspective of the stability of inorganic ABX_3 perovskites used for the construction of solar cells, including the architecture of the devices, the structure of the perovskites, the synthesis and the additives used, as well as the efficiencies achieved and future trends.

2. PEROVSKITE SOLAR CELL DEVICES

The basic structure of PSCs shown in Figure 1, consists of an optically transparent conductive substrate, followed by a "n" type semiconductor layer responsible for the transport of electrons, which are produced in the perovskite layer "i" in which the photoelectric effect takes place. Attached to this is a gap transporter film of a "p" semiconductor and finally a conductive electrode such as gold, carbon or silver. However, it is not

the only structure tested (nip), since type cells have been generated (pin) which are commonly called inverted PSCs, in both cases solar irradiation is carried out through the conductive glass which is commonly oxide of fluorine doped tin (FTO) or indium tin oxide (ITO) although the use of graphene thin films has also been reported. Some researchers have tried irradiating the cells from the conductive electrodes, although this has not presented a competitive photo-conversion efficiency, nevertheless it is important to know that these devices can take advantage of the diffuse radiation that hits the other side of the PSCs [41-46].

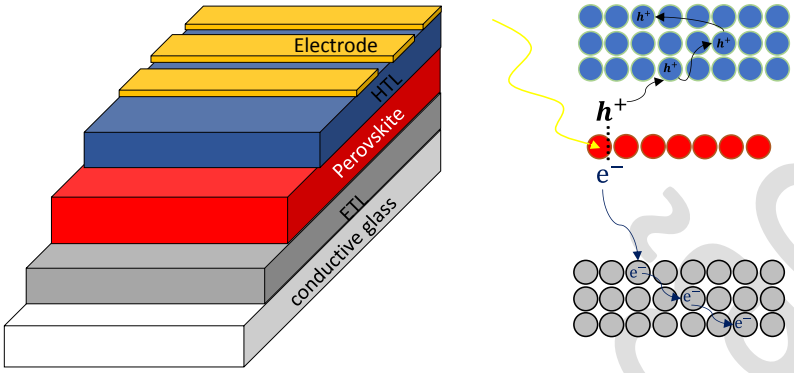

Figure 1: General structure of a PCS.

As already mentioned, the photoelectric effect is carried out on the perovskite, allowing the generation of electric current in these devices. This can be described as the promotion of an electron from the valence band of perovskites to the conduction band, followed by the mobility of electrons and holes (excitons) in opposite directions, being the generation of the exiton or electron hole pair, Equation 1, to later be separated through semiconductor films, said mobility which is expressed by Equations 2 and 3 for the electron in n-type films, while what happened in p-type films is described by Equations 4 and 5 [47, 48].

$$ABX_3 + h\upsilon = (e^- \ldots . h^+)ABX_{3x} \tag{1}$$

Conducting hole across in ETL

$$(e^- \ldots . h^+)ABX_3 = e^-ETL + h^+ABX_3 \tag{2}$$

$$h^+ABX_3 = h^+(HTL) \tag{3}$$

Conducting hole across in HTL

$$(e^- \ldots . h^+)ABX_3 = h^+(HTL) + e^-ABO_3 \tag{4}$$

$$e^-ABX_3 = e^-(ETL) \tag{5}$$

In the general structure of PSCs, a pair of layers are required that can separate the positive and negative charges once the exiton has been generated, as shown in Equations 2-5. This process must be performed quickly, to avoid recombination of electrons, which in turn results in low photoconversion efficiency, these layers of diverse materials must be energetically coupled with the perovskite used to facilitate these processes [49-51], as shown in Figure 2. Load-bearing films can help improve the stability of perovskites, since when placed on the bottom and top they help to isolate the perovskite from external factors, therefore the correct choice of these films allows to extend the life time of these devices. In the case of HTL, there is a large number of possible materials for this purpose, among the most used materials are (2,2′, 7,7′-tetrakis (N, N-di-p-methoxyphenylamine) -9, 9′-spirobifluorene)) (Spiro-OMeTAD) or poly (triarylamine) (PTTA). Another widely used material is Poly (3,4-ethylenedioxythiophene) -poly (styrene sulfonate) (PEDOT: PSS). With the aim of improving these films, modifications have been made to the most widely used films, such as the Spiro-OMeTAD, in which the modification has been reported changing the position of the substituents p-methoxy (-OMe) in ortho positions, goal and for, which allowed to identify, that the position for is the most efficient in terms of transport of holes [3, 41, 52-55].

A molecularly engineered hole transport material with a simple asymmetric fluorene-dithiophene (FDT) core replaced by N, N-di-p-methoxyphenylamine donor groups, may serve as HTL, other promising materials are allotropic forms of carbon as carbon nanotubes, which have been used for this purpose. On the other hand, the use of inorganic structures as hole carriers, such as NiOx, as well as Cu-doped oxides has also been investigated [56-58]. Also, a PSCs structure like Au/Spiro-OMeTAD/$CsPbI_3$/$CsPbBr_3$/TiO_2/FTO has been studied [59-62].

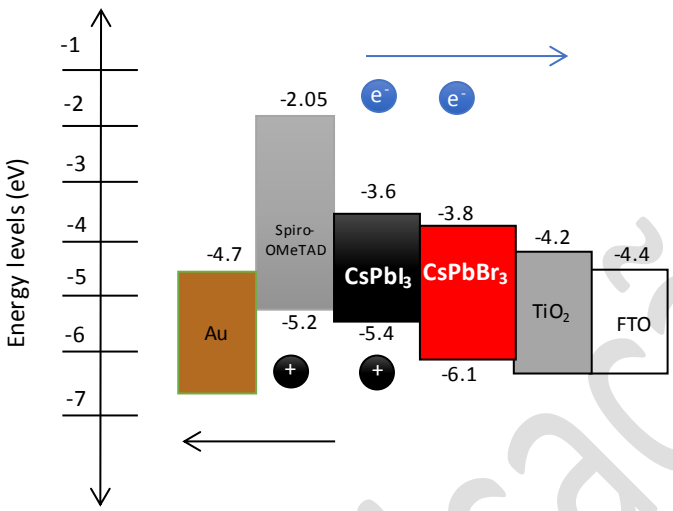

Figure 2: Schematic energy-level diagram of Au/Spiro-OMeTAD/$CsPbI_3$/$CsPbBr_3$/TiO_2/FTO.

It is important to emphasize that the negatively charged carrier must present a band gap capable of preventing the flow of electrons but facilitating the mobility of the holes because the negatively charged particles generated by the photoelectric effect carried out in the perovskite are subtracted dare of n-type semiconductor films, of which the most common is TiO_2, either in its anatase, rutile or even brokite phase, with the purpose of improving ETL. The anatase phase of TiO_2 is the most used as an ETL in perovskite solar cells (DSSC) or as a photoanode in dye-sensitized solar cells (DSSC), using synthetic [63] or natural [64] dyes. with Y has been reported, which has allowed a better adjustment of energy levels to those of perovskite, thus preventing recombination. Other works on materials used as ETL have reported the use of SnO_2 or ZnO, mixtures of metallic oxides, and even the application of organic macromolecules such as fullerene, which has been used alone or decorated with Zn, and the graphene used to doping the TiO_2. In particular, the use of graphene has been shown to stabilize the cubic phase of perovkites, increasing their useful life [49, 65-67].

The perovskite photoactive layer is made up of chemical structures represented by ABX_3 where "A" corresponds to a large cation, such as Cs^+ or methyl ammonium, located in the center of the crystal, "B" is a cation located in the corners commonly Pb^{2+}, although Sn^{2+} has also been used, while "X" corresponds to an anion, particularly I^-, Br^-, Cl^-, located in the center of the edges of the cubic cell [68, 69]. Ideally, perovskites have a cubic crystalline structure centered on the faces, this being the most desired for their photovoltaic applications. However, it is not the only structure that can be formed, since they can also have tetragonal, orthorhombic or rhombohedral phases. To evaluate this, the Goldschmidt's tolerance factor is used (Equation 6), which depends on the ionic radii of cations A and B and on anion X [68, 70]. In Figure 3, the cubic structure of perovskite ABX_3 and some factors of tolerance for various perovskites are shown.

$$t = \frac{r_A + r_B}{\sqrt{2}(r_B + r_x} \tag{6}$$

Where r_A and r_B are the ionic radio of the cations A and B and r_x is the ionic radius of the anion, if this number is equal to 1, the crystal structure will be face-centered cubic, if this value is higher, the structure will be hexagonal, if t is between 0.9 and 1 the crystallography will correspond to a distorted cube, while at values t between 0.7 and 0.9, the perovskite will present a tetragonal structure; on the other hand, at values t less than 0.7, the structures could be orthorhombic and rhombohedral. In other words, when the Goldschmidt tol-

erance factor is different from 1, distortions in the network increase [71-73]. In the case of perovskites for photovoltaic applications in its active phase, also called the black phase, t is required to be greater than 0.8 and less than 1. Likewise, the symmetric cubic phase is obtained when (0.9 < t > 1) or high temperatures. However, perovskites with organic cations such as $FAPbI_3$ (t ≈ 1) or $MAPbI_3$ (t ≈ 0.9) or $CsPbI_3$ (t ≈ 0.8) that have a Goldschmidt's tolerance factor suitable for the black phase, present the inactive phase at room temperature, also called yellow phase [38, 71, 74-76].

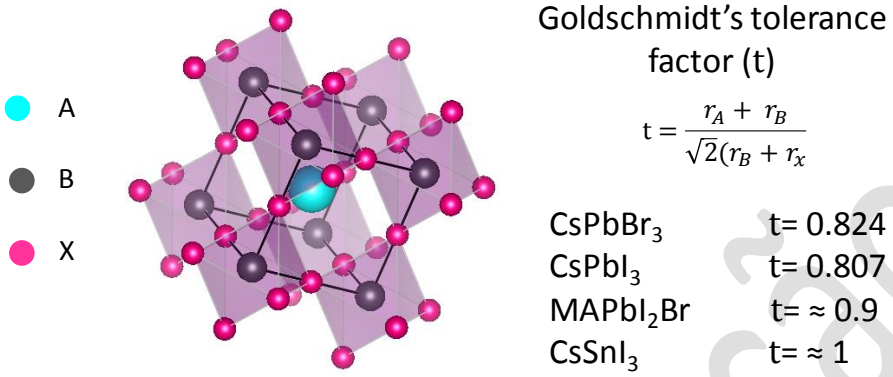

Figure 3: Cubic structure of perovskite ABX_3 and tolerance factors of $CsPbBr_3$, $CsPbI_3$, $CsPbI_2Br$, and $CsSnI_3$ (Drawn with VESTA 3) [77].

As already mentioned, inorganic perovskites have better stability than those with an organic component, which when are irradiated by light generate superoxide O^{2-}, which reacts with the protonated organic component, meanwhile Cs^+, which is the most common substituent "A", lacks protons in its structure, which reduces the effect of superoxide, increasing stability against the effects of light and oxygen, compared to organic componentes. However, for B^{2+} type substituents such as Sn^{2+}, it usually oxidizes to Sn^{4+} and changes the properties of perovskites that contain it [13, 76, 77]. Another adverse effect of environmental conditions is humidity, since it favors the structural rearrangement of inorganic perovskites towards the formation of the δ-orthorhombic inactive phase [78-80]. According to Yihui Li et al., it is possible to maintain this $CsPbI_2Br$ structure for more than 300 hours by keeping the humidity below 25% [22]. A variable to take into account is the temperature, since the photoactive phases are favored at high values, as shown in Figure 4, however, at room temperature the most stable phase (orthorhombic) is photovoltaically inactive [6, 81, 82].

Modification of components A, B or X has been the first route to follow to increase the chemical and structural stability of perovskites, either by the total or partial replacement of any of its components, or by doping that relaxes the structural stress. Efforts have also been focused on optimizing the processes for obtaining these structures, controlling heat treatment, grain size, and the use of both organic and inorganic additives [32, 82-88].

3. STABILITY OF INORGANIC PEROVSKITES

As mentioned, inorganic perovskites have better stability than those with an organic component, which when are irradiated by light generate superoxide O^{2-}, which reacts with the protonated organic component, meanwhile Cs^+, which is the most common substituent "A", lacks protons in its structure, which reduces the effect of superoxide increasing stability against the effects of light and oxygen, compared to organic components, however, for B^{2+} type substituents such as Sn^{2+}, it usually oxidizes to Sn^{4+} and changes the properties of perovskites that contain it [13, 78, 79]. Another adverse effect of environmental conditions is humidity, since it favors the structural rearrangement of inorganic perovskites towards the formation of the δ-orthorhombic inactive phase [80-82]. According to LI *et al.*, it is possible to maintain this $CsPbI_2Br$ structure for more than 300 hours by keeping the humidity below 25% [22]. A variable to take into account is the temperature, since the photoactive phases are favored at high values, as shown in Figure 4. However, at room temperature the most stable phase (orthorhombic) is photovoltaically inactive [6, 83, 84].

Modification of components A B or X has been the first route to follow to increase the chemical and

structural stability of perovskites, either by the total or partial replacement of any of its components, or by doping that relaxes the structural stress. Efforts have also been focused on optimizing the processes for obtaining these structures, controlling heat treatment, grain size, and the use of both organic and inorganic additives [32, 84-90].

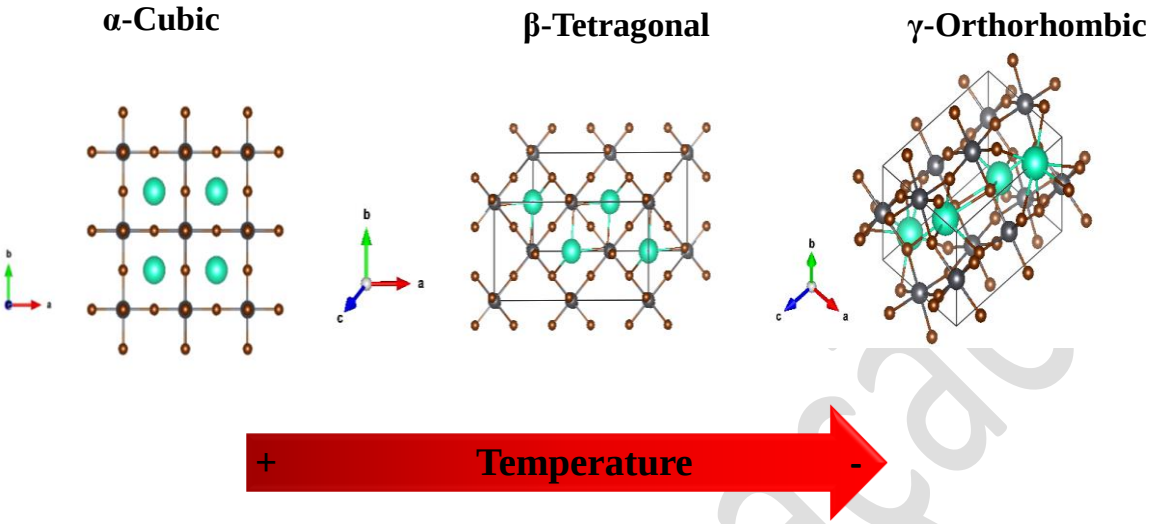

Figure 4: Effect of temperature on the formation of active phases of $CsPbX_3$ inorganic perovskites (Drawn with VESTA 3) [75].

4. METHODS OF OBTAINING ABX_3 PEROVSKITES

The production of both organic and ABX_3 inorganic perovskites for application in solar devices must be carried out in such a way that highly crystalline structures are obtained, which homogeneously coat the surface and present the fewest possible defects, since the quality of the films perovskite has a significant effect on the stability and efficiency of devices. The desirable characteristics of these films can be achieved through control of crystallization, pre-treatments of the precursors, additives or catalysts, the technique of applying the precursors and by the applied heat treatment. In this context, there are various techniques that can be used to obtain high quality films by spin coating technique (using one or two steps) and vapor deposition technique.

4.1 One step technique

The chemical synthesis of the ABX_3 perovskites is carried out by solvating the precursors, in polar media such as Dimethylformamide (DMF) or Dimethyl sulfoxide (DMSO), as well as solvent mixtures, obtaining a precursor solution, which is used to coat a surface and generate the precursor film, using the spin-coating or deep-coating techniques. The use of anti-solvents to promote crystallization and the formation of high-quality films is common, the most commonly used being diethyl ether, toluene and chlorobenzene, followed by a heat treatment that allows the production of perovskite [91-97]. The composition of the precursor solution depends directly on the desired perovskite, if we take the perovskite of $CsPbI_3$ as an example, the use of CsI, PbI_2, as precursors will be required on a molar basis. While the required heat treatment will be up to 300 °C to favor the crystallization of the active phase [20, 98]. WANG *et al.*, prepared the $CsPbI_3$ perovskite in a ratio of solvents (1: 4) DMF:MSO with precursors CsI and PbI_2, 1 M, by means of the spin-coating technique with an annealing temperature of 250 °C [99]. ZHU *et al.*, reported the convenient presence of controlled pores in $CsPbIBr_2$ perovskites using the one-step technique, which provides better crystallinity and fewer film defects allowing cell efficiency of up to 9% [100]. On the other hand, ZHANG *et al.*, studied 6 different anti-solvents; ethyl acetate, toluene, chlorobenzene, chloromethane, isopropanol and diethyl ether for the synthesis of $CsPbIBr_2$, showing the influence of these for crystallization, homogeneity and packing of the grains, as well as to restrict the formation of holes, denoting a better film formation when using diethyl ether [94]. Figure 5 illustrates the two-step technique for making perovskite films.

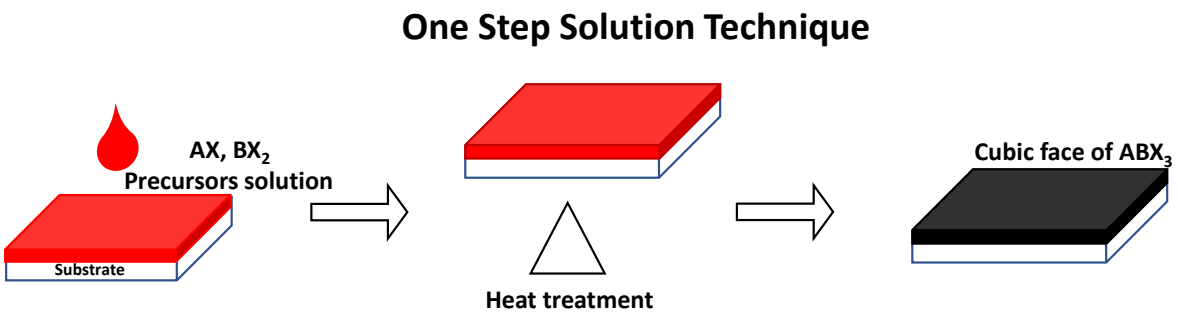

Figure 5: Schematic procedure of the one-step technique for obtaining perovskite films.

4.2 Two Steps Technique

The two-step technique consists in the addition of a first perovskite precursor, generally the precursor of Pb^{2+}, or Sn^{2+} dissolved in DMF or DMSO, by spin-coating for its subsequent drying, followed by the addition of the Cs precursor dissolved in methanol or in another polar solvent, to increase the concentration of said precursor, due to the low solubility that salts like CsBr present in DMF and DMSO, the inclusion of Cs can be done by Spin or Deep coating [18, 101-103]. Once this is done, a heat treatment is carried out whose temperature will depend on the perovskite and the desired phase. LIU *et al.*, reported obtaining the perovskite $CsPbBr_3$ by this technique, dissolving $PbBr_2$ in DMF and then adding this solution on an FTO substrate previously adhered in the spin coater, the coated FTO substrate was dried and dipped in a 30 mg solution of CsBr in methanol, varying the time from 5 to 15 minutes, for its subsequent heat treatment at 180 °C, generating smooth and dense films with excellent stability under atmospheric conditions [104]. The synthesis of $CsPbxSn_{1-x}I_3$ has been reported using the two-step technique, applying a first layer of PbI_2 in DMF by spin-coating followed by immersion for 6 hours in a solution of CsI and SnI_2 in anhydrous methanol, followed by heat treatment at 160 °C, this according to what was reported by TANG *et al*, said perovskite reached a stability in PSCs of up to 30 days [102]. Figure 6 illustrates the two-steps technique for making perovskite films.

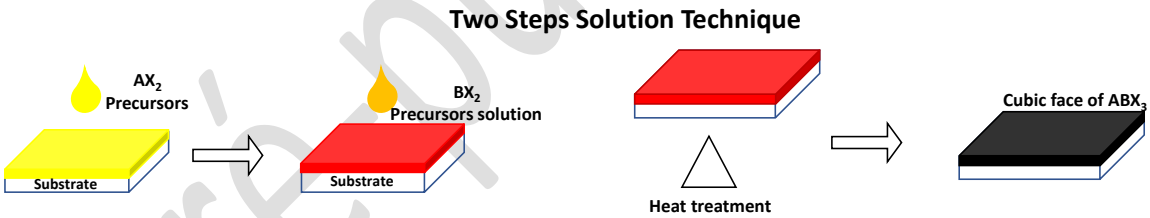

Figure 6: Schematic procedure of the two-steps technique for obtaining perovskite films.

4.3 Vacuum processing

Vapor deposition is a technique used to obtain perovskite ABX_3 films that does not have the limitations of the solubility limits of solution techniques (one and two-step techniques), in addition to allowing more precise control of the thickness of the films generated, the homogeneity of perovskites, grain limits and their reproducibility [27, 105-107]. In 2017 *FROLOVA et al.*, reported obtaining a compact and homogeneous 300 nm layer by means of the co-evaporation technique using CsI and PbI_2 as precursors for obtaining $CsPbI_3$ with excellent photochemical and thermal properties [108]. LI et al., reported obtaining $CsPbBr_3$ / $CsPb_2Br_5$ perovskites by precisely controlling the film thickness of the precursor materials [109]. Another technique assisted by steam is the sequential vapor deposition, which consists of forming a first layer of CsX precursor, to later cover it with PbX_2, efficiently controlling the thickness of the resulting perovskite, this technique was used by TONG *et al.*, who with his workgroup obtained $CsPbBr_3$ perovskite with controlled grain sizes and passivation of grain boundaries, in addition to improving cargo carrier transport and achieving 45% controlled humidity stability for over 2000 hours) [28]. LUO *et al.*, obtained $CsPbBr_3$ by means of the assisted evaporation of Br on the perovskite of $CsPbI_3$, obtaining in a first stage the perovskite $CsPbI_3$ by means of the one-step technique, followed by the exchange of halogen by the assisted evaporation of Br [23]. Co-evaporation vacuum process (A) and vapor assisted deposition technique (B) for making perovskite films are

shown in Figure 7.

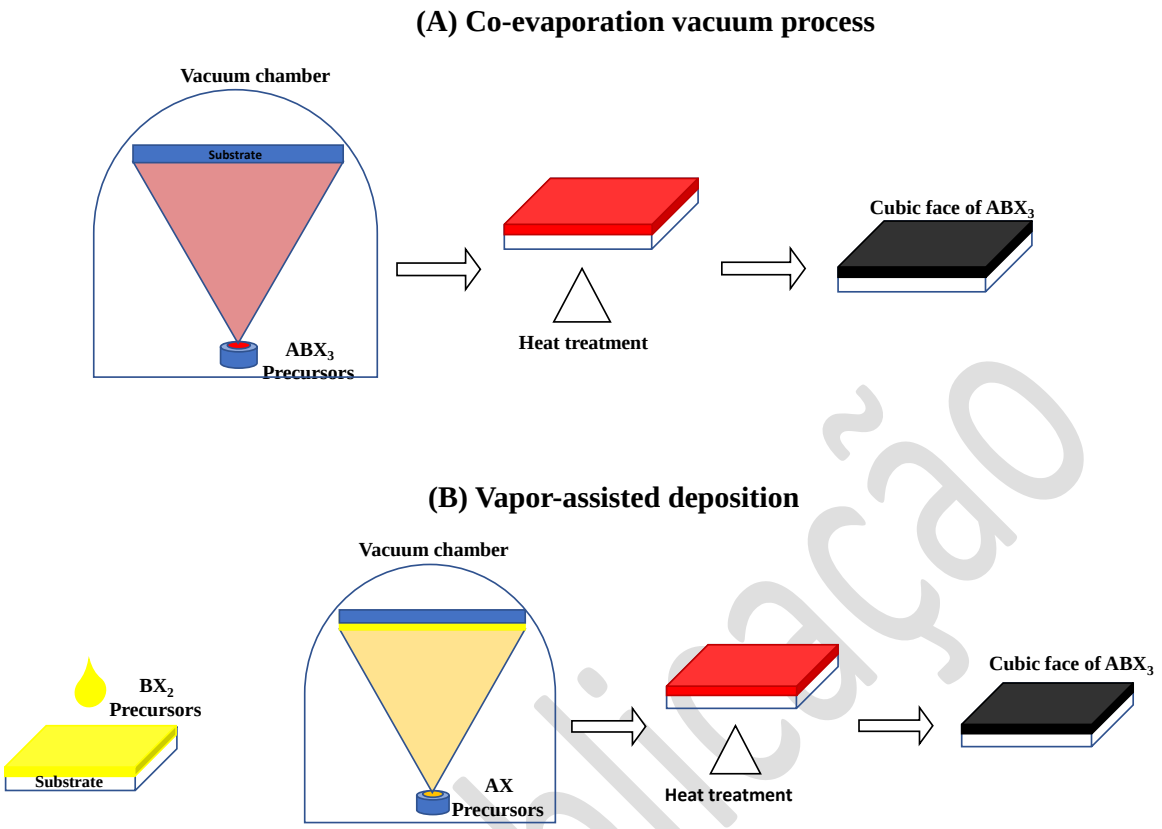

Figure 7: Co-evaporation vacuum process (A) and vapor assisted deposition technique (B) for making perovskite films.

5. INORGANIC PEROVSKITES

The inorganic perovskites that show the best efficiencies in PSCs, like hybrid perovskites, have the cation of Pb^{2+} as substituent B, while Cs^{+} is the most used substituent A, in addition, they present the best results in terms of efficiency. On the other hand, the halides used are I, Cl or Br. Next, an analysis of the stability and efficiency of solar cells of the perovskites $CsPbI_3$, $CsPbBr_3$, $CsPbBrI_2$, $CsPbBr_2I$, and $CsSnX_3$, which have better optical properties, as well as greater stability in the crystal structure, is presented.

5.1 Pure $CsPbI_3$, and $CsPbBr_3$ perovskites

The inorganic perovskite of $CsPbI_3$ is the one with the highest efficiency in PSCs so far, with a record that exceeds 18% efficiency. The high efficiency values achieved using this structure are due to the optical band gap of ~ 1.73 eV. The absorption that this perovskite presents has been reported between 700 and 750 nm in its active phase [75], ideal for photovoltaic applications, despite this, the cubic phase is not very stable at room temperature, once obtained at high temperatures it presents a rapid rearrangement of its structure by decreasing temperature, passing through three photoactive black phases, α-cubic, β- tetragonal, γ- ortho-rhombic and finally decaying to the inactive yellow phase δ-orthorhombic, the latter the most stable at room temperature, this it is explained by the low tolerance factor of Goldschmidt that the α phase presents, which is 0.807, just above the minimum limits necessary to formalize the perovskite [22, 26, 33, 71, 110].

The inorganic perovskite of $CsPbBr_3$, for its part, has proven to be a structure of greater stability than its $CsPbI_3$ counterpart, with a tolerance factor of 0.824. This perovskite has greater stability under environmental conditions, its active phase has a reddish coloration, so the absorption of this compound ranges between 520 and 550 nm in its cubic phase, in addition to presenting an optical band gap of 2.3 eV, which declines up to 4 eV, once it is completely degraded. The temperature required to obtain the cubic phase of this perovskite has been reported between 250 °C and 350 °C [28, 106, 111, 112].

Various works have focused on maintaining the cubic phase for as long as possible, investigating the

method of obtaining it, controlling the dimensions, the inclusion of various substituents in A and B as dopants, or the use of protective films (encapsulation) to delay atmospheric effects, or the use of carbon as a conductive electrode as a hydrophobic barrier [45, 113, 114].

5.2 $CsPbI_3$ perovskite

The use of HI or $HPbI_3$ as a precursor in the method of obtaining one and two steps, has been shown to improve the stability of the active phase of perovskite $CsPbI_3$ and allow it to be obtained at lower temperatures [25], XIANG *et al.*, reported obtaining $CsPbI_3$ using HI as a catalyst, which allowed the generation of stable perovskite for 2 months and 300 hours under irradiation, using carbon as the conductive electrode [98]. In the work reported by XU *et al.*, they use 4 (1H) -pyridinethione as an additive to promote crystallization through the interaction of S-Pb, which allows obtaining this α-cubic perovskite at low temperature (90-100 ° C) and keep it stable for 20 days, with a cell efficiency of 85%, compared to the first day of testing [115].

ZHANG *et al.*, reported obtaining $CsPbI_3$ with a stability of 1000 hours. Obtained by using phenyl-C61-butyric acid methyl ester in mixture with chlorobenzene, as an antisolvent, it used methylammonium iodide as a mediator, since it allows to improve the quality of the films, and it is removed by heat treatment at 350 °C, generating PSCs with up to 16% efficiency [75]. Another additive used during the synthesis of this perovskite is phenylethylammonium iodide which hinders the transition to the inactive phase thanks to the steric effect of the additive once the crystals have formed [20]. Choline iodine was reported to stabilize perovskite and improve its electronic communication with the electron transport layer in the work presented by WANG *et al.*, who built a PSCs using this additive; It remained stable at lighting for 500 h, with only a loss of 5% of its efficiency [24]. The use of SCN^- as an additive to stabilize the perovskite α-$CsPbI_3$ was reported by YAO *et al.*, who compared to the perovskite obtained without the catalyst reported an increase in efficiency from 15.36 to 17.04%, as well as indicating that perovskite with additive took longer to progress to the yellow orthorhombic phase [85]. CHEN et al., obtaining highly efficient $CsPbI_3$ Quantum Dots (QD) based PSCs using mesoscopic TiO_2 as the ETM; they reported a fabricated device with the best PCE value reaching 14.32% (reverse scan) combined with an unprecedented high current density at short crcuit (J_{s-c}) of 17.77 mA cm^{-2} [116].

5.3 $CsPbBr_3$ perovskite

In the work reported by ZHANG *et al.*, passivation of perovskite film defects was achieved using the ionic liquid 1-butyl-2, 3-dimethylimidazolium chloride, improving efficiency up to 61.3% compared to that obtained without the ionic additive, the perovskite obtained with the additive, maintained a stability under relative humidity of 70% at 20 ° C for 30 days with carbon as a conductive electrode [117]. Another additive used to promote the quality of perovskite crystals is the application of $BiBr_3$, prior to the application of the CsBr coating in the two-step technique, reported by PEI *et al.*, who obtained a stability of 90% PCE per 1000 h. using a carbon electrode [118].

WANG *et al.*, obtained the perovskite $CsPbBr_3$ by the two-step technique and using NH_4SCN as additive in the precursor solution of $PbBr_2$, followed by immersion in CsBr in methanol, generating a dense and homogeneous film with a stability of the cells greater than 200 hours under lighting [119]. BU *et al.*, reported obtaining this perovskite using the two-step technique, which was assembled in an HTL-free cell; the carbon used as an electrode was modified with polyaniline / graphite, which gave it a stability of up to 50 days at 80% relative humidity, with a 47% higher efficiency than unmodified carbon cells, this stability is attributed to the effect of the carbon modified as a better hydrophobic insulator [120].

XIANG *et al.*, prepared by vapor deposition the perovskite of $CsPbBr_3$ applying a first treatment of 320 ° C for 20 minutes, followed by a second treatment for 40 minutes at different temperatures, finding that a second treatment of 300 ° C achieves higher efficiency, coupled with excellent thermal stability of 40 days stored at 100 °C [27]. Table 1 presents a relationship of the architecture of different PSCs cells based on perovskites $CsPbI_3$ and $CsPbBr_3$, their stability and efficiency.

Table 1: Performance and stability time of PSCs with $CsPbI_3$ and $CsPbBr_3$ perovskites.

Architecture	Testing or storage time	J_{SC} (mA*cm^2)	V_{OC} (V)	FF %	PCE %	Reference
$CsPbI_3$						
FTO/TiO_2/ $CsPbI_3$/Carbon	60 storage days	18.5	0.79	69.0	9.5	[98]
FTO/ TiO_2/ $CsPbI_3$/PTAA/Au	60 storage days	18.95	1.059	75.1	15.07	[20]
FTO/PPTA/ $CsPbI_3$/ PCBM layer/Ag	20 storage days	17.38	1.08	73.67	13.88	[115]
FTO/ TiO_2/ $CsPbI_3$/Spiro-OMeTAD/Au	500 hours of testing	20.03	1.11	82	18.4	[24]
FTO/ TiO_2/ $CsPbI_3$/PTAA/Au	Not reported	20.34	1.09	77	17.04	[8]
ITO/SnO_2/ $CsPbI_3$/ Spiro-OMeTAD/Au	1000 hours of testing	20.1	1.06	75.3	16.04	[75]
FTO/ TiO_2/$CsPbI_3$/Spiro-OMeTAD/Au	100 hours of testing	17.77	0.84	Not reported	14.32	[116]
$CsPbBr_3$						
FTO/ TiO_2/$CsPBr_3$/ Mixed-carbon	30 storage days	7.16	1.357	72.97	7.09	[113]
FTO/ TiO_2/$CsPbBr_3$/Spiro-OMeTAD/Au	60 storage days	7.71	1.37	81	8.65	[106]
FTO/ TiO_2/$CsPbBr_3$/Carbon	30 storage days	7.45	1.61	83	9.92	[117]
FTO/ TiO_2/$CsPbBr_3$/Carbon	1000 hours of testing	7.84	1.39	80	8.73	[118]
ITO/ TiO_2/$CsPbBr_3$/Spiro-OMeTAD/Au	200 hours of testing	7.76	1.375	79.31	8.47	[119]
FTO/ TiO_2/$CsPbBr_3$/Carbon	50 storage days	6.87	1.59	81.21	8.87	[120]
FTO/ TiO_2/$CsPbBr_3$/Carbon	40 storage days	7.37	1.545	82.2	9.35	[27]

J_{SC} = Current density at short circuit; V_{OC} = Voltage at open circuit; FF = Fill factor; PCE = Power-conversion efficiency

5.4 Halide mixture in CsPb perovskite

The band gap of 1.73 eV of its own and $CsPbI_3$ is ideal for use as an adsorbent layer in PSCs, however its low thermal stability limits its long-term application in these devices [75]. On the other hand, the perovskite of $CsPbBr_3$ is more stable under normal atmospheric conditions it presents a band gap of 2.3 eV [118], so the combination in different proportions of the halides I and Br in the structures allows to combine the intrinsic properties of these semiconductors, and allow to substantially improve the stability thus as a greater absorption of the electromagnetic spectrum. The $CsPbIBr_2$ perovskite has an absorption around 600 nm with 2.05 eV optical band gap, as well as a stability superior to that of the ABI_3 perovskites and a better efficiency than the $ABBr_3$ perovskites, which exceed 12% [103,121]. For its part, the perovskite composed with $CsPbI_2Br$ further reduces its energy gap by around 1.9 eV and it improves its thermal stability, although to a lesser extent than its $CsPbIBr_2$ counterpart with an absorbance close to 650 nm and efficiencies greater than 16% [19, 57, 122]. For these reasons year after year more work is done focused on improving both the properties of these absorbent layers and their performance in PSCs. It should be clarified that both structures can be obtained by following the same procedures as singles halide perovskites.

In an effort to increase the stability of the absorbing layer, NiO_x and CeO_x charge transport films were used to isolate the perovskite $CsPbIBr_2$ from the effects of humidity and temperature according to what was reported by YANG *et al.;* they reported that this dispositive achieved stability for 500 hours (stored at 45-50% of humidity) [123]. ZHU *et al.*, obtained a perovskite of $CsPbBr_3$ using the one-step technique followed by the addition of CsI in methanol to obtain $CsPbIBr_2$ methodology that allowed obtaining a film that presented few limits grain, high crystallinity and that in cell allowed to maintain 90% of the conversion efficiency for 60 days in environmental conditions of humidity and temperature [124]. ZHANG *et al.*, synthesized the $CsPbIBr_2$ perovskite using the one-step technique, using diethyl ether as an anti-solvent and a guanidinium additive to passivate the structure defects, obtaining a perovskite with a stability of 100 hours and an efficiency of 9.17%, which is high for this structure [94]. As already mentioned, the TiO_2 antasa phase is the semiconductor that has been most used as ETL in PSCs, it is used as a TiO_2 compact film (c-TiO_2) or as a TiO_2 mesoporous film (m-TiO_2), a photoactive inorganic perovskite of $CsPbI_2Br$ on TiO_2 films was deposited

using a gradiente thermal annealing method (GTA) [125, 126] and PCE values of 14.5% and 16.07% were obtained, while PCE values of 15.25% and 15.69% were obtained when doping the $CsPbI_2Br$ perovskite with In^{3+} and Eu^{2+}cations [127, 128]. Some researchers report that precalating the glass-FTO/c-TiO_2 substrate at 90 °C and using tammonium hexafluorophosphate (NH_4PF_6) as precursor additive to modify the grain size of the $CsPbI_2Br$ perovskite it is possible to obtain a photovaitaic device with an efficiency of 10.1% [129]. On the other hand, tin oxide (SnO_2) has been used as ETL in solar cells containing $CsPbI_2Br$ perovskite and using ethyl acetate as anti-solvent or a programmable crystallization method to obtaining PCE values from 14.33 % to 16.58% andy J_{sc} values from 13.61 to 16.23 $mAcm^{-2}$ [130-132]. LIU *et al.*, obtained the inorganic perovskite of $CsPbIBr_2$ by means of the two-step technique assisted by vapor deposition, using copper (II) phthalocyanine (CuPC) and carbon as an electrode transporting film, which provides better stability to both perovskite and the device in general resisting for one month at 60 °C [107]. Table 2 collects results from works reported for PSCs in which the stability as a function of perovskite storage or test time of $CsPbIBr_2$ and $CsPbI_2Br$ can be seen.

Table 2: Performance and stability time of PSCs with $CsPbI_2Br$ and $CsPbIBr_2$.

Architecture	Testing or storage time	J_{SC} ($mA*cm^2$)	V_{OC} (V)	FF %	PCE %	Reference
FTO/NiO_x/$CsPbIBr_2$/ZnO@C_{60}/Ag	10 hours of testing	15.1	1.1	75.5	12.6	[133]
FTO/TiO_2/ $CsPbIBr_2$/Spiro-OMeTAD/Au	100 hours of testing	10.24	1.2	74.6	9.17	[94]
FTO/TiO_2/$CsPbIBr_2$/CuPc/Carbon	720 hours of testing	9.65	1.236	63.1	8.76	[107]
ITO/NiO_x/$CsPbIBr_2$/CeO_x/Ag	500 hours of testing	8.76	1.01	63.35	5.60	[123]
FTO/TiO_2/$CsPbIBr_2$/Carbon	60 days of storage	10.71	1.169	66	9.16	[124]
FTO/TiO_2/$CsPbI_2Br$/PCBM/Ag	500 hours of testing	15.33	1.22	78.8	14.78	[134]
FTO/c-TiO_2/m-TiO_2/$CsPbI_2Br$/ Spiro-OMeTAD /Ag	3 hours of testing	15.8	1.27	78.0	15.5	[125]
ITO/c-TiO_2/$CsPbI_2Br$/Spiro-OMeTAD /Au	120 hours of testing	16.79	1.23	77.81	16.07	[126]
FTO/c-TiO_2/m-TiO_2/Doped-$CsPbI_2Br$/ CuSCN/rGO/Au	>1600 hours of testing	15.91	1.28	74.85	15.27	[127]
FTO/TiO_2/$CsPbI_2Br$/Spiro-OMeTAD/Au	30 storage days in air	15.44	1.25	79.00	15.25	[128]
ITO/SnO_2/$CsPbI_2Br$/Spiro-OMeTAD/Ag	25 storage days in N_2 atmosphere	16.23	1.21	76.29	15.07	[130]
ITO/SnO_2:C_{60}-EDA/$CsPbI_2Br$/Spiro-OMeTAD/MoO/Ag	65 storage days in dry air	15.41	1.34	80.30	16.58	[131]
ITO/ ZnO:Cs_2CO_3/ $CsPbI_2Br$/PCBM/Ag	200 hours of testing	16.34	1.28	78.42	16.42	[97]
FTO/NiO_x/$CsPbIBr_2$/ZnO@C_{60}/Ag	300 hours of testing	15.2	1.14	77	13.3%	[121]
ITO/SnO_2-ZnO/ $CsPbIBr_2$/Spiro-OMeTAD -MoO_3/Ag	360 hours of testing	15	1.23	78.8	14.16	[122]
ITO/SnO_x/ $CsPbIBr_2$/ Poly (DTSTPD-r-BThTPD)Au	900 hours of intermittent testing	14.25	1.4	77	15.53	[135]
FTO/TiO_2/ $CsPbIBr_2$/ Spiro-OMeTAD/Au	1000 hours of testing	15.32	1.32	83.29	16.79	[93]
ITO/ZnO/ $CsPbIBr_2$/ Spiro-OMeTAD/Ag	2.5 hours of testing at 200 °C	14.9	1.22	75.3	13.7	[87]
PDOT:PSS/Al:ZnO/$CsPbIBr_2$/tBCA/PTAA/MoO_3/Ag	60 storage days	15.87	1.26	75.41	15.08	[136]

J_{SC} = Current density at short circuit; V_{OC} = Voltage at open circuit; FF = Fill factor; PCE = Power-conversion efficiency; CuSCN = Copper thiocyanate; C_{60}-EDA = Fullerene-ethylenediamine; rGO = Reduced graphene oxide

The synthesis of $CsPbI_2Br$ by the one-step technique using DMSO ducts, which allows the formation of

large-grain films with low defect density, and a longer life time for charge carriers, as well as better stability of up to 500 h according with GUANNAN *et al.* [135]. The use of $CaCl_2$ as an additive in the formation of the $CsPbI_2Br$ perovskite by the one-step technique allows obtaining more stable structures with a prohibited band of 1.91 eV as well as good performance in PSCs, reaching a competitive efficiency of 16.79%, which is maintained at 90% after 1000 hours of continuous testing [93]. Processing at low temperatures is feasible to obtain perovskite as demonstrated by Xia Yang and his team, who obtained the absorbent layer by the one-step method at 120 ° C. This was used to assemble a flexible cell which reached an efficiency 15% maximum that declined 7, 9 and 86% after 60 days stored under environmental conditions, 360 hours at 85 ° C and 30 h at 65% humidity, respectively. The cell structure was formed using tert-butyl cyanoacetate (T-BCA), PTTA and MoO_3 as gap carriers, ZnO_2 aluminum doped and PEDOT: PSS as gap carriers [136].

Thermal stabilization and optimization of $CsPbI_2Br$-based PCSs have also been tested by applying ZnO_2 doped with Cs_2CO_3 as an electron-bearing film that allows a good extraction of these charge carriers, resulting in an increase in efficiency, coupled with the isolation of perovskite that increases its stability ZnO: Cs_2CO_3 maintains efficiency at 93% for 200h. vs 73% who maintained the device that used only ZnO_2 [97]. Another film used to improve electron transport is ZnO_2 @ C_{60} which in 2018 achieved a photoconversion efficiency of 13.3% with a stability that reached 360 hours with only 20% loss of initial efficiency [59], results comparable to those presented by YAN *et al.*, who reported a stability of 300 hours with a loss of 15% of the photoconversion efficiency (14.16%) using SnO_2-ZnO as an electron carrier [122]. For his part, GOU *et al.*, reported the device based in CsPbI2Br, the poly [(dithiene [3,2-b: 2 ', 3'-d] silolethiene [3,4-c] pyrrole-4,6-dione) -random- (2,2'- bithiophenethiene [3,4-c] pyrrole-4,6-dione) (poly (DTSTPD-r-BThTPD)) (and as an electron acceptor $SnCl_2$ device that reached a PCE of 15.53% and remained under intermittent illumination for 900 h, maintaining 71% of the initial efficiency [135]. In general, a greater number of works focused on $CsPbI_2Br$ are reported due to their lower bandgap. that allows obtaining greater efficiencies in PSCs although they have less stability, on the other hand, $CsPbIBr_2$ have better stability but less efficiency, so much of the effort is focused on increasing efficiency.

5.5 $CsSnX_3$ perovskite

In the search to obtain lead-free perovskites, the use of Sn^{2+} has been tried to substitute it, since said element presents serious damage to the environment, thus the $CsSnI_3$, $CsSnBr_3$ and $CsSnCl_3$ perovskites are presented as a greener option than their counterparts. These include lead, these structures have an optical band interval along the near and visible infrared region, with absorbance at 750, 610 and 420, respectively. However, Sn^{2+} has short periods of functionality as a photoactive layer due to a rapid oxidation of Sn^{2+} to Sn^{4+}. In the case of the perovskite $CsSnI_3$, it has a band gap of 1.3 eV, which is ideal for its application in photovoltaic cells [40, 89, 137-139]. In this sense, ZHANG *et al.*, stabilized the $CsSnI_3$ perovskite in a reducing environment by using cobaltocene, which is a large electron donor, which prevents Sn^{2+} oxidation, which results in increased stability of $CsSnI_3$, however, it presents a low efficiency of 3%, however this is an encouraging result to replace lead in these devices [137]. The highest efficiency reported so far for $CsSnI_3$ is 5.03% obtained by WANG *et al.* To do this, they synthesized perovskite in a single step using triphenyl phosphite as an antioxidant additive to stabilize perovskite, which allowed its analysis under illumination for 400 minutes, which is considerable for this type of perovskites [140]. Another work on the development of cells based on perovskite $CsSnI_3$ is that reported by ZHU *et al.*, who obtained the perovskite $CsSnI_3$ using the evaporative assisted solution method. The photovoltaic device had a maximum yield of 2.23% and an average yield of 1.93% that presented a decay at 70% of its initial efficiency at 70% humidity, after 60 min [141]. LEI *et al.*, synthesized the perovskite $CsPb_xSn_{1-x}I_3$, with a band gap between 1.3 and 1.7 eV observing a better electrical conductivity when increasing the Sn^{2+} concentration; although they did not build cells, their research provides an applicability option to these devices with a lower concentration of lead [110, 142].

The perovskite $CsSnBr_3$ presents a band gap value around 1.9 eV, a thermal stability higher than 437 °C and a transition to its inactive phase that takes 48 hours at room temperature and around 60% humidity [143]. However, its preparation using additives such as SnF_2 has allowed $CsSnBr_3$ to be obtained with an optical band gap of 1.73 eV by reducing the gap between the valence band and the fermi level, coupled with limiting the formation of Sn^{2+} to Sn^{4+} [145]. SABBA *et el.*, reported PSCs of this structure prepared without SnF_2 and with this additive, demonstrating that the efficiency increases slightly from 0.1 to 0.91%, in turn they observed that if Br^- is included in the perovskite of $CsSnI_3$ the efficiency improves reporting a maximum efficiency of 1.67% for the perovskite $CsSnIBr_2$, the latter with a prohibited band of 1.75 eV [144]. ISLAM *et al.*, synthesized the perovskite $CsSnCl_3$ in order to improve its optoelectronic properties, since this structure has a band gap of 2.8 eV, which rules it out of applications in photovoltaic cells, so by including metals such as Cr or Mn sought to increase absorption in the visible spectrum, demonstrating that the valence band of Mn-

doped $CsSnCl_3$ samples shifts slightly towards the region of highest energy, which facilitates the promotion of electrons towards the conduction band, showing better photoconductivity and greater absorption than pure perovskite from $CsSnCl_3$ [86].

Table 3: Performance and stability time of PSCs of $CsSnX_3$.

Architecture	Testing or storage time	J_{SC} (mA*cm^2)	V_{OC} (V)	FF %	PCE %	Reference
FTO/TiO_2/Al_2O_3/ $CsSnI_3$/NiO/Carbon	100 hours of storage	18.24	0.36	46	3.0	[137]
FTO/TiO_2/$CsSnIBr_2$/Al_2O_3/$CsSnI_3$/Carbon	9 hours of testing	17.4	0.31	57	3.2	[143]
ITO/PEDOT:PSS/$CsSnI_3$/PCBM/Ag	30 days of storage under N_2	23.792	0.42	No reported	4.13	[140]
ITO/ TiO_2/ $CsSnI_3$/ Spiro-OMeTAD:TBP/Au	No reported	27.67	0.201	29	1.66	[144]
ITO/ TiO_2/ $CsSnI_2Br$/Spiro-OMeTAD:TBP/Au	No reported	15.06	0.289	38	1.67	[144]
ITO/ TiO_2/ $CsSnIBr_2$/ Spiro-OMeTAD:TBP/Au	No reported	11.57	0.311	43	1.56	[144]
ITO/ TiO_2/ $CsSnI_3$/ Spiro-OMeTAD: TBP/Au	No reported	3.99	0.410	58	0.95	[144]

J_{SC} = Current density at short circuit; V_{OC} = Voltage at open circuit; FF = Fill factor; PCE = Power-conversion efficiency

Great efforts have been focused on optimizing the fabrication processes of solar cells with different structures based on ABX_3 inorganic perovskites, using different methods like spin coating and vacuum deposition, controlling heat treatment, grain size of the photoactive phase, and the use of both organic and inorganic additives with the aim to get photovoltaic diapositives with high efficiency (PCS), filled factor (FF), open circuit voltage (Voc), and short circuit current density (Jsc) with high stability under environmental conditions of temperature and moisture. Table 4 show a summary of the best solar cells based on inorganic perovskite obtained until now; the three inorganic halide perovskites solar cells that present the best values of efficiency at high testing time are $CsPbI_3$, $CsPbIBr_2$, and $CsPb_2Br$, with the architectures of FTO/TiO_2/$CsPbI_3$/Spiro-OMeTAD/Au, FTO/TiO_2/$CsPbIBr_2$/Spiro-OMeTAD/Au, and FTO/c-TiO_2/m-TiO_2/Doped-$CsPbI_2Br$/ CuSCN/rGO/Au, respectively.

Table 4: PSCs made with ABX_3 inorganic halide perovskites with the higher effciciency and testing time.

Architecture	Testing or storage time	J_{SC} (mA*cm^2)	V_{OC} (V)	FF %	PCE %	Reference
FTO/ TiO_2/ $CsPbI_3$/Spiro-OMeTAD/Au	**500 hours of testing**	**20.03**	**1.11**	**82**	**18.4**	[24]
FTO/ TiO_2/ $CsPbI_3$/PTAA/Au	Not reported	20.34	1.09	77	17.04	[8]
FTO/TiO_2/ $CsPbIBr_2$/ Spiro-OMeTAD/Au	**1000 hours of testing**	**15.32**	**1.32**	**83.29**	**16.79**	[93]
ITO/SnO_2:C_{60}-EDA/$CsPbI_2Br$/Spiro-OMeTAD/MoO/Ag	65 storage days in dry air	15.41	1.34	80.30	16.58	[131]
ITO/ ZnO:Cs_2CO_3/ $CsPbI_2Br$/PCBM/Ag	200 hours of testing	16.34	1.28	78.42	16.42	[97]
ITO/c-TiO_2/$CsPbI_2Br$/ Spiro-OMeTAD /Au	120 hours of testing	16.79	1.23	77.81	16.07	[126]
ITO/SnO_2/ $CsPbI_3$/ Spiro-OMeTAD/Au	1000 hours of testing	20.1	1.06	75.3	16.04	[75]
FTO/c-TiO_2/m-TiO_2/Doped-$CsPbI_2Br$/ CuSCN/rGO/Au	**> 1600 hours of testing**	**15.91**	**1.28**	**74.85**	**15.27**	[127]

6. CONCLUSIONS

Inorganic perovskites are a promising alternative to supply the most widely used organometallic perovskites for the development of solar cells, so the focus of this review was to know the factors that affect these structures, the methods of obtaining them, the architecture with which photovoltaic devices, their components and processes of generation and load mobility are manufactured, as well as trends to improve both stability and efficiency. In this work we compile the photoconversion efficiencies reported in different investigation reports, as well as the stability that these devices present under light irradiation or due to their storage time, under different conditions of temperature and humidity. Various studies carried out to adjust the perovskite band gap to improve its capacity as an adsorbent film, by doping or substitution of metal cations A^+ and B^{2+}, or by mixing halides I^- and Br^-, were analyzed. The techniques used to stabilize the photoactive phases of perovskites, which range from the method of obtaining, the use of additives, heat treatments, the composition of perovskites, the application of various materials as charge carriers, mainly inorganic, which manage to stabilize the active phase. On the other hand, the use of carbon as an electrode generates a hydrophobic layer that stabilizes the PSCs and time of use and storage is increased. The total substitution of Pb in the perovskite structures is also addressed since, due to the contamination that this element causes to the environment. In general, inorganic perovskites can considerably improve their performance using all these considerations, being the halides mixture the most common route promising to achieve an efficient and stable structure, so a large number of papers show increasing interest in the use of $CsPbI_{x-y}Br_y$ perovskites, and cell components to optimize these devices.

7. ACKNOWLEDGMENTS

Cristian M. Díaz Acosta acknowledges CONACYT for the scholarship (446796). Antonia Martinez-Luevanos thanks Universidad Autonoma de Coahuila in Mexico for the financial support for this research.

8. CONFLICTS OF INTEREST

The authors have no conflicts of interest to declare.

9. BIBLIOGRAPHY

[1] SASKI, M., PROCHOWICZ, D., MARYNOWSKI, W., *et al.*, "Mechanosynthesis, optical, and morphological properties of MA, FA, Cs-SnX_3 (X = I, Br) and phase-pure mixed-halide $MASnI_xBr_{3-x}$ perovskites", *European journal of inorganic chemistry*, v. 2019, n. 22, pp. 2680–2684, 2019.

[2] YU, H., RYU, J., LEE, J.W., *et al.*, "Large grain-based hole-blocking layer free planar-type perovskite solar cell with best efficiency of 18.20%", *ACS Applied materials & interfaces*, v. 9, n. 9, pp. 8113–8120, 2017.

[3] CHEN, W., WU, Y., YUE, Y., *et al.*, "Efficient and stable large-area perovskite solar cells with inorganic charge extraction layers", *Science*, v. 350, n. 6263, pp. 944–948, 2015.

[4] XU, X., WANG, Z., YU, J., *et al.*, "Phase engineering for highly efficient quasi-two-dimensional all-inorganic perovskite light-emitting diodes via adjusting the ratio of Cs cation", *Nanoscale research letter*, v. 14. n. 255, pp. 1-8, 2019.

[5] GARCÍA-FERNANDEZ, A., BERMÚDEZ-GARCÍA, J.M., CASTRO-GARCÍA, S., *et al.*, "Phase transition, dielectric properties, and ionic transport in the $[(CH_3)_2NH_2]PbI_3$ organic-inorganic hybrid with 2H-hexagonal perovskite structure", *Inorganic chemistry*, v. 56, n. 9, pp. 4918–4927, 2017.

[6] YANG, Z., SURRENTE, A., GALKOWSKI, K., *et al.*, "Impact of the halide cage on the electronic properties of fully inorganic cesium lead halide perovskites", *ACS Energy letters*, v. 2, n. 7, pp. 1621–1627, 2017.

[7] NENON, D.P., CHRISTIANS, J.A, WHEELER, L.M, *et al.*, "Structural and chemical evolution of methylammonium lead halide perovskites during thermal processing from solution", *Energy & environmental science*, v. 9, n. 6, pp. 2072–2082, 2016.

[8] KOJIMA, A., TESHIMA, K., SHIRAI, Y., *et al.*, "Organometal halide perovskites as visible-light sensitizers for photovoltaic cells", *Journal of the american chemical society*, v. 131, n. 17, pp. 6050–6051, 2009.

[9] SEOK, S. I., GRÄTZEL, M., PARK, N.G., "Methodologies toward highly efficient perovskite solar cells", *Nano-micro small*, v. 14, n. 20, pp. 1704177 (1-17), 2018.

[10] HWANG, T., YUN, A.J, KIM, J., KIM, J., *et al.*, "Electronic traps and their correlations to perovskite solar cell performance via compositional and thermal annealing controls", *ACS Applied materials & interfaces*, v. 11, n. 7, pp. 6907–6917, 2019.

[11] HSIAO, K.C., JAO, M.H., LI, B.T., *et al.*, "Enhancing efficiency and stability of hot casting p–i–n perovskite solar cell via dipolar ion passivation", *ACS Applied Energy Materials*, v. 2, n. 7, pp. 4821–4832, 2019.

[12] JIANG, C.S., YANG M., ZHOU, Y., *et al.*, "Carrier separation and transport in perovskite solar cells studied by nanometre-scale profiling of electrical potential", *Nature communications*, v. 6, n. 8397, pp. 1-10, 2015.

[13] SENOCRATE, A., ACARTÜRK, T., KIM, G.Y., *et al.*, "Interaction of oxygen with halide perovskites". *Journal of Materials Chemistry* A., v. 6, n. 23, pp.10847–10855, 2018.

[14] TARGHI, F.F., JALILI, Y.S., KANJOURI, F., "$MAPbI_3$ and $FAPbI_3$ perovskites as solar cells: Case study on structural, electrical and optical properties", *Results in physics*, v. 10, n. 4, pp. 616–627. 2018.

[15] LUO, W., WU, C., WANG, D., *et al.*, "Efficient and stable perovskite solar cell with high open-circuit voltage by dimensional interface modification". *ACS Applied Materials & Interfaces*, v. 11, n. 23, pp. 9149–9155, 2019.

[16] SVEINBJÖRNSSON, K., "Preparation and characterization of lead halide perovskites towards sustainable, cost-effective and upscalable solar cell manufacture", Degree Ph.D., Uppsala University. Uppsala, Sweden, 2018.

[17] MALI, S.S., PATIL, J.V., HONG, C.K., "Simultaneous improved performance and thermal stability of planar metal ion incorporated $CsPbI_2Br$ all-inorganic perovskite solar cells based on MgZnO nanocrystalline electron transporting layer", *Advanced Energy Materials*, v. 10, n. 3, pp.1–13, 2020.

[18] TANG, K.C., YOU, P., YAN, F., "Highly stable all-inorganic perovskite solar cells processed at low temperature", *Solar RRL*, v. 2, n. 8, pp. 1-5, 2018.

[19] WANG, J., ZHANG, J., ZHOU, Y., *et al.*, "Highly efficient all-inorganic perovskite solar cells with suppressed non-radiative recombination by a Lewis base", *Nature communications*, v. 11, n. 1, pp. 1–9, 2020.

[20] WANG, K., JIN, Z., LIANG, L., *et al.*, "All-inorganic cesium lead iodide perovskite solar cells with stabilized efficiency beyond 15%", *Nature communications*, v. 9, n. 1, pp. 4544, 2018.

[21] LI Y, WANG Y, ZHANG T, *et al.*, "Li dopant induces moisture sensitive phase degradation of an all-inorganic $CsPbI_2Br$ perovskite", *Chemical communications*, v. 54, n. 70, pp. 9809–9812, 2018.

[22] HU, Y., BAI, F., LIU, X., *et al.*, "Bismuth incorporation stabilized α-$CsPbI_3$ for fully inorganic perovskite solar cells", *ACS Energy letters.*, v. 2, n. 10, pp. 2219–2227, 2017.

[23] LUO, P., ZHOU, Y., ZHOU, S., *et al.*, "Fast anion-exchange from $CsPbI_3$ to $CsPbBr_3$ via Br_2-vapor-assisted deposition for air-stable all-inorganic perovskite solar cells", *Chemical engineering j*ournal, v. 343, n. 1, pp. 146–154. 2018.

[24] WANG, Y., DAR, M., ONO, L.K., *et al.*, "Thermodynamically stabilized b-$CsPbI_3$–based perovskite solar cells with efficiencies >18%", *Science*, v. 365, n. 6453, pp. 591–595, 2019.

[25] LIAO, J.F., RAO, H.S., CHEN, B.X., *et al.*, "Dimension engineering on cesium lead iodide for efficient and stable perovskite solar cells", *Journal of materials chemistry A*., v. 5, n. 5, pp. 2066–2072, 2017.

[26] WANG, P., ZHANG, X., ZHOU, Y., *et al.*, "Solvent-controlled growth of inorganic perovskite films in dry environment for efficient and stable solar cells", *Nature commun*ications, v. 9, n. 1, pp. 1-7. 2018.

[27] XIANG, T., ZHANG, Y., WU, H., *et al.*, "Universal defects elimination for high performance thermally evaporated $CsPbBr_3$ perovskite solar cells", *Solar energy materials and solar cells*, v. 7, n. 110317, pp.1-7, 2020.

[28] TONG, G., CHEN, T., LI, H., *et al.*, "Phase transition induced recrystallization and low surface potential barrier leading to 10.91%-efficient $CsPbBr_3$ perovskite solar cells", *Nano energy*, v. 65, n. 104015, pp. 1-10 2019.

[29] WANG, K.L., WANG, R., WANG, Z.K., *et al.*, "Tailored phase transformation of $CsPbI_2Br$ films by copper(II) bromide for high-performance all-Inorganic perovskite solar cells", *Nano lett*ers, v. 19, n. 8, pp. 5176–5184, 2019.

[30] YANG, B., WANG, M., HU, X., *et al.*, "Highly efficient semitransparent $CsPbIBr_2$ perovskite solar cells via low-temperature processed In_2S_3 as electron-transport-layer", *Nano Energy*, v. 57, n. 4, pp. 718–727, 2019.

[31] LI, X., TAN, Y., LAI, H., *et al.*, "All-inorganic $CsPbBr_3$ perovskite solar cells with 10.45% efficiency by evaporation-assisted deposition and setting intermediate energy levels", *ACS Applied materials & interfaces*, v. 11, n. 33, pp. 29746–29752, 2019.

[32] ZHANG, L., LI, B., YUAN, J., *et al.*, "High-voltage-efficiency inorganic perovskite solar cells in a wide solution-processing window", *The journal of physical chemistry letters*, v. 9, n. 13, pp. 3646–3653, 2018.

[33] NAM, J.K., JUANG, M.S., CHAI, S.U., *et al.*, "Unveiling the crystal formation of cesium lead mixed-halide perovskites for efficient and stable solar cells", *The journal of physical chemistry letters*, v. 8, n. 13, pp. 2936–2940, 2017.

[34] LAU, C.F.J., DENG, X., MA, Q., *et al.*, "$CsPbIBr_2$ perovskite solar cell by spray-assisted deposition", *ACS Energy letters*, v. 1, n. 3, pp. 573–577, 2016.

[35] NAM, J.K., CHAI, S.U., CHA, W., *et al.*, "Potassium incorporation for enhanced performance and stability of fully inorganic cesium lead halide perovskite solar cells". *Nano lett*ers, v. 13, n. 3, pp. 2028–2033, 2017.

[36] AJJOURI. E.Y., CHIRVONY, V.S., SESSOLO, M., *et al.*,"Incorporation of potassium halides in the mechanosynthesis of inorganic perovskites: feasibility and limitations of ion-replacement and trap passivation", *RSC Advances*, v. 8, n. 72, pp. 41548–41551, 2018.

[37] SUN, H., ZHANG, J., GAN, X., *et al.*, "Pb-reduced $CsPb_{0.9}Zn_{0.1}I_2Br$ thin films for efficient perovskite solar cells", *Advanced energy materials*, v. 9, n. 25, pp. 1–9, 2019.

[38] YE, Q., ZHAO, Y., UM, S., *et al.*, "Stabilizing the black phase of cesium lead halide inorganic perovskite for efficient solar cells", *Science China chemistry*, v. 62, n. 7, pp. 810–821, 2019.

[39] LI, X., BI, D., YI, C., *et al.*, "A vacuum flash−assisted solution process for high-efficiency large-area perovskite solar cell ", *Science*, v. 353, n. 6294, pp. 58-62. 2016.

[40] CHEN, Z., WANG, J.J., REN, Y., *et al.*, "Schottky solar cells based on $CsSnI_3$ thin-films", *Applied physics letters.*, v. 101, n. 9, pp. 1-5, 2012.

[41] KATO, Y., FUJIMOTO, S., KOZAWA, M., *et al.*, "Maximum efficiencies and performance-limiting factors of inorganic and hybrid perovskite solar cells", *Physical review applied*, v. 12, n. 2, pp. 12:1–16. 2019.

[42] AHN, N., JEON, I., YOON, J., *et al.*, "Carbon-sandwiched perovskite solar cell", *Journal of materials Chemistry A*, v. 6, n. 4. pp. 1382–1389, 2018.

[43] HUANG, Y., "Modeling of perovskite solar cells, III-V optoelectronic devices and Kelvin probe microscopy", Degree Ph.D. INSA de Rennes, Français, 2018.

[44] SONG, Z., WATTHAGE, S.C., PHILLIPS, A.B., *et al.*, "Pathways toward high-performance perovskite solar cells: review of recent advances in organo-metal halide perovskites for photovoltaic applications", *Journal of photonics for energy*, v. 6, n. 2, pp. 1-24. 2016.

[45] CONG M, YANG B, CHEN J, *et al.*, "Carrier multiplication and hot-carrier cooling dynamics in quantum-confined $CsPbI_3$ perovskite nanocrystals", *The journal of physical chemistry letters*, v. 11, n. 5, pp.1921–1926, 2020.

[46] ZHANG. J., BAI, D., JIN, Z., *et al.*, "3D – 2D – 0D interface profiling for record efficiency all-inorganic $CsPbBrI_2$ perovskite solar cells with superior stability", *Advanced energy materials*, v. 8, n. 5, pp. 1-9, 2018.

[47] KIRCHARTZ, T., BISQUERT, J., MORA-SERO, I., *et al.*, "Classification of solar cells according to mechanisms of charge separation and charge collection", *Physical Chemistry Chemical Physics*, v. 17, n. 6, pp. 4007-4014, 2017.

[48] BAKR, Z.H., WALI, Q., FAKHARUDDIN, A., *et al.*, "Advances in hole transport materials engineering for stable and efficient perovskite solar cells", *Nano energy*, v. 34, pp. 271-305, 2017.

[49] KOGO, A., SANEHIRA, Y., NUMATA, Y., *et al.*, "Amorphous metal oxide blocking layers for highly efficient low-temperature brookite TiO_2-based Perovskite solar cells", *ACS Applied materials & interfaces*, v. 10, n. 3, pp. 2224–2229, 2018.

[50] EPERON, G.E., BURLAKOV, V.M., DOCAMPO, P., *et al.*, "Morphological control for high performance, solution-processed planar heterojunction perovskite solar cells" *Advanced functional materials*, v. 24, n. 1, pp. 151–157, 2014.

[51] MCMEEKIN, D.P., SADOUGHI, G., REHMAN, W., *et al.*, "Support-a mixed-cation lead halide perovskite absorber for tandem solar cells", *Science*, v. 351, n. 6269, pp. 151–155, 2016.

[52] NG, C.H., RIPOLLES, T.S., HAMADA, K., *et al.*, "Tunable open circuit voltage by engineering inor-

ganic cesium lead bromide/iodide perovskite solar cells", *Scientific reports*, v. 8, n. 1, pp. 1-10, 2018.

[53] LEE, J.W., NA, S.I., KIM, S.S., "Efficient spin-coating-free planar heterojunction perovskite solar cells fabricated with successive brush-painting", *Journal of power sources*, v. 339, n. 5, pp. 33-40, 2017.

[54] YAVARI, M., MAZLOUM-ARDAKANI, M., GHOLIPOUR, S., *et al.*, "Carbon nanoparticles in high-performance perovskite solar cells", *Advanced energy Materials*., v. 8, n. 12, pp. 1–8, 2018.

[55] KIM, J.H., LIANG, P.W., WILLIAMS, S.T., *et al.*, "High-performance and environmentally stable planar heterojunction perovskite solar cells based on a solution-processed copper-doped nickel oxide hole-transporting layer", *Advanced mater*ials, v. 27, n. 8, pp. 695–701, 2015.

[56] SALIBA, M., ORLANDI, S., MATSUI, T., *et al.*, "A molecularly engineered hole-transporting material for efficient perovskite solar cells", *Nature energy*., v. 1, n. 2, pp. 1-7, 2016.

[57] LIU. C., LI, W., ZHANG, *et al.*, "All-inorganic $CsPbI_2Br$ Perovskite solar cells with high efficiency exceeding 13%", *Journal of the american chemical society*, v. 140, n. 11, pp. 3825–3828, 2018.

[58] ARORA, N., DAR, M.I., HINDERHOFER, *et al.*, "Perovskite solar cells with CuSCN hole extraction layers yield stabilized efficiencies greater than 20%", *Science*, v. 358, n. 6364, pp. 358:768–771, 2017.

[59] TIEN, C.H., CHEN, L.C., LEE. K.Y., *et al.*, "High-quality all-inorganic perovskite $CsPbBr_3$ quantum dots emitter prepared by a simple purified method and applications of light-emitting diodes", *Energies*, v. 12, n. 18, pp. 1-13, 2019.

[60] HAO, F., STOUMPOS, C.C., CAO, D.H., *et al.*, "Lead-free solid-state organic-inorganic halide perovskite solar cells", *Nature photonics*, v. 8, n. 6, pp. 489-494, 2014.

[61] BIAN, H., BAI, D., JIN, Z., *et al.*, "Graded Bandgap $CsPbI_{2+x}Br_{1-x}$ Perovskite Solar Cells with a Stabilized Efficiency of 14.4%", *Joule*, v. 2, n. 8, pp. 1500–1510, 2018.

[62] HASSAN, A.K., CHAURE, N.B., RAY, A.K., *et al.*, "Structural and electrical studies on sol-gel derived spun TiO_2 thin films", *Journal of physics D: applied physics*., v. 36 n. 9, pp. 1120–1125, 2003.

[63] SANTOS-SOUZA, A.P., CAVALCANTE N.M., AGUIAR-FREIRE, F.N., *et al.*, "Performance evolution of titanium oxide deposited by electrophoresis in photoelectrodes of dye -sensitized solar cells", *Matéria (Rio J.)* v.26, n.1, pp. 1-14, 2021.

[64] AMARAL-AMANCIO, M., RAPHAEL E., ROMAGUERA-BARCELAY, Y., *et al.*, "Natural days from amazon forest: potential application in dye-sensitized solar cells", *Matéria (Rio J.)* v.26, n.2, pp. 1-11, 2021.

[65] YANG, Y., WANG, T., ZHANG, Y., *et al.*, "High performance all-inorganic $CsPbI_2Br$ perovskite solar cells with low energy losses", *Solar energy*, v. 196 n. 10, pp. 22–26, 2020.

[66] MA, J., SU, J., LIN, Z., *et al.*, "Improve the oxide/perovskite heterojunction contact for low temperature high efficiency and stable all-inorganic $CsPbI_2Br$ perovskite solar cells", *Nano energy*, v. 67, pp. 104241, 2020.

[67] WU, Y., YANG, X., CHEN, H., *et al.*, "Highly compact TiO_2 layer for efficient hole-blocking in perovskite solar cells", *Applied physics express*, v. 7, n, 5, pp. 1-5, 2014.

[68] PAL, P., SAHA, S., BANIK, A., *et al.*, "All-solid-state mechanochemical synthesis and post-synthetic transformation of inorganic perovskite-type halides", *Chemical-A european journal*, v. 24, n. 8, pp. 1811–1815 2018.

[69] PEEDIKAKKANDY, L., BHARGAVA, P., "Composition dependent optical, structural and photoluminescence characteristics of cesium tin halide perovskites", *RSC Advances*, v. 6, n. 24, pp. 19857–19860, 2016.

[70] YAO, M.M., JIANG, C.H., YAO, J.S., *et al.*, "General synthesis of lead-free metal halide perovskite colloidal nanocrystals in 1-dodecanol", *Inorganic Chemistry*, v. 58, n. 17, pp. 11807–11818, 2019.

[71] GUVENC, C.M., YALCINKAYA, Y., OZEN, S., *et al.*, "Gd^{3+}-doped α-$CsPbI_3$ nanocrystals with better phase stability and optical properties", *The journal of physical chemistry C*, v. 123 n. 40, pp. 24865–24872, 2019.

[72] TSUI, K.Y., ONISHI, N., BERGER, R.F., "Tolerance factors revisited : geometrically designing the ideal environment for perovskite dopants", *The journal of physical chemistry C*, v. 120, n. 40, pp. 23293–23298, 2016.

[73] SATO, T., TAKAGI, S., DELEDDA, S., *el al.*, "Extending the applicability of the Goldschmidt tolerance factor to arbitrary ionic compounds", *Scientific reports*, v. 6, n. 1, pp. 1–10. 2016.

[74] SIDDIQUE-SUBHANI, W., WANG, K., DU, M., *et al.*, "Goldschmidt-rule-deviated perovskite

$CsPbIBr_2$ by barium substitution for efficient solar cells", *Nano energy*, v. 61, n. 2, pp. 165-172, 2019.

[75] ZHANG, T., WANG, F., CHEN, H., *et al.*, "Mediator–antisolvent strategy to stabilize all-Inorganic $CsPbI_3$ for perovskite solar cells with efficiency exceeding 16%", *ACS energy letters*, v. 5, n. 5, pp. 1619–1627 2020.

[76] STOUMPOS C.C, MALLIAKAS, C.D, KANATZIDIS, M.G., "Semiconducting tin and lead iodide perovskites with organic cations: Phase transitions, high mobilities, and near-infrared photoluminescent properties", *Inorganic chemistry*, v. 52, n. 15, pp. 9019–9038, 2013.

[77] MOMMA, K., IZUMI, F., "VESTA 3 for three-dimensional visualization of crystal, volumetric and morphology data," *Journal of applied crystallogr*aphy, v. 44, n. 1, pp. 1272-1276, 2011.

[78] ZHOU, Y., ZHAO, Y., "Chemical stability and instability of inorganic halide perovskites", *Energy & environmental science*, v. 12, n. 5, pp. 1495–1511, 2019.

[79] ANAYA, M., GALISTEO-LÓPEZ, J.F., CALVO, M.E., et al., "Origin of light-induced photophysical effects in organic metal halide perovskites in the presence of oxygen", *The journal of physical chemistry letters*, v. 9, n. 14, 3891–3896, 2018.

[80] YANG, S., WANG, Y., LIU, P., *et al.*, "Functionalization of perovskite thin films with moisture-tolerant molecules", *Nature Energy*, v.1, n. 2, pp. 1–7, 2016.

[81] IDÍGORAS, J., APARICIO, F.J., CONTRERAS-BERNAL, L., *et al.*, "Enhancing moisture and water resistance in perovskite solar cells by encapsulation with ultrathin plasma polymers", *ACS Applied materials & interfaces*, v. 10, n. 14, pp. 11587–11594, 2018.

[82] RONG, Y., HOU, X., HU, Y., *et al.*, "chloride and moisture on perovskite crystallization for efficient printable mesoscopic solar cells", *Nature communications*, v. 33, n. 4. pp. 647-648, 2017.

[83] MARRONNIER, A., ROMA G., BOYER-RICHARD, S., *et al.*, "Anharmonicity and disorder in the black phases of $CsPbI_3$ used for stable inorganic perovskite solar cells", *ACS Nano*, v. 12, n. 4, pp. 3477–3486, 2018.

[84] YUN, R., LUO, L., HE, J., *et al.*, "Mixed-solvent polarity-assisted phase transition of cesium lead halide perovskite nanocrystals with improved stability at room temperature", *Nanomaterials*, v. 9, n. 11, pp. 1-12, 2019.

[85] YAO, Z., JIN, Z., ZHANG, X., *et al.*, "Pseudohalide (SCN^-)-doped $CsPbI_3$ for high-performance solar cells", *Journal of Materials Chemistry C*, v. 7, n. 44. pp.13736–13742, 2019.

[86] ISLAM, J., HOSSAIN, A.K.M.A., "Narrowing band gap and enhanced visible-light absorption of metal-doped non-toxic $CsSnCl_3$ metal halides for potential optoelectronic applications", *RSC Adv*ances, v. 10, n. 13 pp. 7817–7827, 2020.

[87] MALI, S.S., PATIL, J.V., HONG, C.K., "Hot-air-assisted fully air-processed barium incorporated $CsPbI_2Br$ perovskite thin films for highly efficient and stable all-inorganic perovskite solar cells", *Nano let*ters, v. 19, n. 9. pp. 6213–6220, 2019.

[88] WOJCIECHOWSKI, K., SALIBA, M., LEIJTENS, T., *et al.*, "Sub-150 °C processed meso-superstructured perovskite solar cells with enhanced efficiency", *Energy & environmental science*, v. 7, n. 3, pp. 1142–1147, 2014.

[89] HEO, J.H., KIM, J., KIM, H., *et al.*, "Roles of SnX_2 (X = F, Cl, Br) additives in tin-based halide perovskites toward highly efficient and stable lead-free perovskite solar cells", *The journal of physical chemistry let*ters, v. 9, n. 20, pp. 6024–6031, 2018.

[90] AJJOURI Y.E., PALAZON, F., SESSOLO, M., *et al.*, "Single-source vacuum deposition of mechanosynthesized inorganic halide perovskites", *Chemistry of materials*, v. 9, n. 20, pp. 7423–7427, 2018.

[91] HOU S, XIE A, XIE Z, *et al.*, BIROWOSUTO, M.D., WANG, H., "Concurrent inhibition and redistribution of spontaneous emission from all inorganic perovskite photonic crystals", *ACS Photonics*, v. 6, n. 6, pp. 1331–1337, 2019.

[92] DONG, C., HAN, X., ZHAO, Y., *et al.*, "A green anti-solvent process for high performance carbon-based $CsPbI_2Br$ all-inorganic perovskite solar cell", *Solar RRL*., v. 2, n. 9. pp. 1800139(1-8), 2018.

[93] HAN, Y., ZHAO, H., DUAN, C., *et al.*, "Controlled n-doping in air-stable $CsPbI_2Br$ perovskite solar Cells with a record efficiency of 16.79%", *Advanced functional mater*ials, v. 30, n. 12. pp. 1-8, 2020.

[94] ZHANG, B., BI, W., WU, Y., *et al.*, "High-performance $CsPbIBr_2$ perovskite solar cells: Effectively promoted crystal growth by antisolvent and organic ion strategies", *ACS Applied materials & interfaces*, v. 11, n. 37. pp. 33868–33878, 2019.

[95] SHI, J., WANG, Y., ZHAO, Y., "Inorganic $CsPbI_3$ perovskites toward high-efficiency photovoltaics", *Energy & environmental materials*, v. 2, n. 2, pp. 73-78, 2019.

[96] MA, J., GUO, X., ZHOU, L., *et al.*, "Enhanced planar perovskite solar cell performance via contact passivation of TiO_2/perovskite interface with NaCl doping approach", *ACS Applied energy materials*, v. 1, n. 8, pp. 3826–3834, 2018.

[97] SHEN, E.C., CHEN, J.D., TIAN, Y., *et al.*, "Interfacial Energy level tuning for efficient and thermostable $CsPbI_2Br$ perovskite solar cells", *Advanced Science*, v. 7, n. 1, pp. 1–9, 2020.

[98] XIANG, S., FU, Z., LI, W., *et al.*, "Highly Air-Stable Carbon-Based α-$CsPbI_3$ Perovskite Solar Cells with a Broadened Optical Spectrum", *ACS Energy lett*ers, v. 3, n. 8, pp. 1824–1831, 2018.

[99] WANG, P., ZHANG, X., ZHOU, Y., et al., "Solvent-controlled growth of inorganic perovskite films in dry environment for efficient and stable solar cells", *Nature commun*ications, v. 9, n. 1, pp. 1–8, 2018.

[100] ZHU, W., ZHANG, Z., CHAI, W., *et al.*, "Benign pinholes in $CsPbIBr_2$ absorber film enable efficient carbon-based, all-inorganic perovskite solar cells", *ACS Applied energy materials*, v. 2, n. 7, pp- 5254–5262, 2019.

[101] CHA, J-H., NOH, K., YIN, W., *et al.*, "Formation and encapsulation of all-inorganic lead halide perovskites at room temperature in metal-organic frameworks", *The journal of physical chemistry letter*, pp. 2270–2277, 2019.

[102] TANG, X., ZHOU, H., PAN, X., *et al.*, "All-inorganic halide perovskite alloy nanowire network photodetectors with high performance", *ACS Applied materials & interfaces*, v. 12, n. 4, pp. 4843–4848, 2020.

[103] AAMIR, M., ADHIKARI, T., SHER, M., *et al.*, "Fabrication of planar heterojunction $CsPbBr_2I$ perovskite solar cells using ZnO as an electron transport layer and improved solar energy conversion efficiency", *New journal of Chem*istry, v. 42, n. 17, pp. 14104–14110, 2018.

[104] LIU, D., HU, Z., HU, W., *et al.*, "Two-step method for preparing all-inorganic $CsPbBr_3$ perovskite film and its photoelectric detection application", *Materials letters*, v. 186, n. 1. pp. 243–246, 2017.

[105] DING, X., REN, Y., WU, Y., *et al.*, "Sequential deposition method fabricating carbonbased fully-inorganic perovskite solar cells", *Science China mater*ials, v. 61, n. 1, pp. 73–79, 2018.

[106] LI, J., GAO, R., GAO, F., *et al.*, " Fabrication of efficient $CsPbBr_3$ perovskite solar cells by single-source thermal evaporation", *Journal of alloys and compounds*., v. 818, n. 3., pp. 152903, 2020.

[107] LIU, X., LI, J., LIU, Z., *et al.*, "Vapor-assisted deposition of $CsPbIBr_2$ films for highly efficient and stable carbon-based planar perovskite solar cells with superior V_{oc}", *Electrochimica acta*, v. 330, n. 1, pp. 135266, 2020.

[108] FROLOVA, L.A., ANOKHIN, D.V., PIRYAZEV, A.A., *et al.*, "Highly efficient all-inorganic planar heterojunction perovskite solar cells produced by thermal coevaporation of CsI and PbI_2", *The journal of physical chemistry letters*, v. 8, n. 1, pp. 6–11. 2017.

[109] LI. H., TONG. G., CHEN. T., *et al.*, "Interface engineering using a perovskite derivative phase for efficient and stable $CsPbBr_3$ solar cells", *Journal of materials chemistry A*, v. 6. n. 29, pp. 14255–14261, 2018.

[110] LEI, T., LAI, M., KONG, Q., *et al.*, "Electrical and optical tunability in all-inorganic halide perovskite alloy nanowires", *Nano Lett*ers, v. 18, n. 6, pp. 3538–3542, 2018.

[111] CHRISTODOULOU, S., STASIO F.D., PRADHAN, S., *et al.*, "High-open-circuit-voltage solar cells based on bright mixed-halide $CsPbBrI_2$ perovskite nanocrystals synthesized under ambient air conditions", *The journal of physical Chemistry C*, v. 122, n. 14, pp. 7621–7626, 2018.

[112] HUANG, H., BODNARCHUK, M.I., KERSHAW. S.V., *et al.*, "Lead halide perovskite nanocrystals in the research spotlight: stability and defect tolerance", *ACS Energy Letters*, v. 2, n. 9, pp. 2071–2083, 2017.

[113] MI, L., ZHANG, Y., CHEN, T., *et al.*, "Carbon electrode engineering for high efficiency all-inorganic perovskite solar cells", *RSC Adv*ances, v. 10, n. 21, 12298–12303, 2020.

[114] CHU, W., SAIDI, W.A., ZHAO, J., *et al.*, "Soft lattice and defect covalency rationalize tolerance of β-$CsPbI_3$ perovskite solar cells to native defects", *Angewandte Chemie*, v. 132, n. 16, pp. 6497–6503, 2020.

[115] XU, X., ZHANG, H, LI, E., *et al.*, "Electron-enriched thione enables strong Pb-S interaction for stabilizing high quality $CsPbI_3$ perovskite films with low-temperature processing", *Chemical science*, v. 11, n. 20, pp. 3132–3140, 2020.

[116] CHEN, K., JIN, W., ZHANG, Y., *et al.*, "High efficiency mesoscopic solar cells using $CsPbI_3$ perovskite quantum dots enabled by chemical interface engineering", *Journal of the american chemical society*, v.

142, n. 8, pp. 3775–3783, 2020.

[117] ZHANG, W., LIU, X., HE, B., *et al.*, "Interface engineering of imidazolium ionic liquids toward efficient and stable $CsPbBr_3$ perovskite solar cells", *ACS Applied materials & interfaces*, v. 12, n. 4, pp. 12, 4540–4548 2020.

[118] PEI, Y., GUO, H., HU, Z., *et al.*, "$BiBr_3$ as an additive in $CsPbBr_3$ for carbon-based all-inorganic perovskite solar cell", *Journal alloys and compounds*, v. 835, n. 9, pp. 155283, 2020.

[119] WANG, D., LI, W., DU, Z., *et al.*, "Highly efficient $CsPbBr_3$ planar perovskite solar cells via additive engineering with NH_4SCN", *ACS Applied materials & interfaces*, v. 12, n. 9, pp. 10579–10587, 2020.

[120] BU, F., HE, B., DING, Y., *et al.*, "Enhanced energy level alignment and hole extraction of carbon electrode for air-stable hole-transporting material-free $CsPbBr_3$ perovskite solar cells", *Solar energy materials and solar cells*, v. 205, n. 9, pp. 110267, 2020.

[121] LIU, C, LI, W., ZHANG, C., *et al.*, "All-inorganic $CsPbI_2Br$ perovskite solar cells with high efficiency exceeding 13%", *Journal of the american chemical society*, v. 140, n. 11, pp. 3825–3828, 2018.

[122] YAN, L., XUE, Q., LIU, M., *et al.*, "Interface Engineering for All-Inorganic $CsPbI_2Br$ Perovskite Solar Cells with Efficiency over 14%", *Advanced mater*ials, v. 30, n. 33. pp. 1–7, 2018.

[123] YANG, J., ZHANG, Q., XU, J., *et al.*, "All-inorganic perovskite solar cells based on $CsPbIBr_2$ and metal oxide transport layers with improved stability" *Nanomaterials*, v. 9, n. 12, pp. 1-10, 2019.

[124] ZHU, W., ZHANG, Q., CHEN, D., *et al.*, "Intermolecular Exchange Boosts Efficiency of Air-Stable, Carbon-Based All-Inorganic Planar $CsPbIBr_2$ Perovskite Solar Cells to Over 9%", *Advanced energy mater*ials, v. 8. n. 30, pp. 1–11, 2018.

[125] LONG, Y., LIU, K., ZHANG, Y., et al., "Ambient air temperature assisted crystallization for inorganic $CsPbI_2Br$ perovskite solar cells", *Molecules*, v. 26, n. 11, pp.1-13, 2021.

[126] CHEN, W., CHEN, H., XU, G., et al., "Precise control of crytal growth for highly effcient $CsPbI_2Br$ perovskite solar cells", *Joule*, v. 3, pp. 191-204, 2019.

[127] MALI, S.S., PATIL, J.V., Steele, J.A., et al., "Implementing dopant-free hole-transporting layers and metal-incorporated $CsPbI_2Br$ for stable all-inorganic perovskite solar cells", *ACS Energy letters*, v. 6, n. 2, pp. 778-788, 2021.

[128] YANG, S., ZHAO, H., HAN Y., et al., "Europium and acetate co-doping strategy for developing stable and efficient $CsPbI_2Br$ perovskite solar cells", *Nano-micro small*, v. 15, n. 46, pp. 1-9, 2019.

[129] PAN, J., ZHANG, X., ZHENG, Y., et al., "Morphology control of perovskite film for efficient $CsPbIBr_2$ based inorganic perovskite solar cells", *Solar energy materials and solar cells*, v. 221, pp. 110878 (1-8), 2021.

[130] ZHANG, F., MA, Z., HU, T., et al., "Ultra-smooth $CsPbI_2Br$ film via programmable crystallization process for high-effciency inorganic perovskite solar cells", *Journal of materials science & technology*, v. 66, pp. 150-156, 2021.

[131] DUAN, CH., LI, J., LIU, Z., et al., "Highly electroluminescent and stable inorganic $CsPbI_2Br$ perovskite solar cell enabled by balanced charge transfer", *Chemical engineering journal*, v. 417, 128053, 2021.

[132] ZHANG, X., YANG, J., XIE, L., et al., "Boosting the performance of low-temperature processed $CsPbI_2Br$ planar perovskite solar cell by interface engineering", *Dyes and pigments*, v. 186, 109024, 2021.

[133] PAN, L., LIU, C., ZHU, H., WAN, M., LI, Y., MAI, Y., "Fine modification of reactively sputtered NiO_X hole transport layer for application in all-inorganic $CsPbI_2Br$ perovskite solar cells", *Solar energy*, v. 196, n. 1, pp. 521–529, 2020.

[134] YIN, G., ZHAO, H., JIANG, H., YUAN, S., NIU, T., ZHAO, K., LIU, Z., LIU, S.(F)., "Precursor Engineering for All-Inorganic $CsPbI_2Br$ Perovskite Solar Cells with 14.78% Efficiency", *Advanced functional mater*ials, v. 28, n. 39, pp. 1–10, 2018.

[135] GUO, Z., JENA, A.K., TAKEI, I., *et al.*, "V_{oc} over 1.4 V for amorphous tin oxide-based dopant-free $CsPbI_2Br$ perovskite solar cells", *Journal of the american chemical society*, v. 142, n. 21, pp. 9725–9734, 2020.

[136] YANG, X., YANG, H., HU, X., *et al.*, "Low-temperature interfacial engineering for flexible $CsPbI_2Br$ perovskite solar cells with high performance beyond 15%", *Journal of materials chemistry A*, v. 8, n. 10, pp. 5308–5314, 2020.

[137] ZHANG, T., LI, H., BAN, H., *et al.*, "Efficient $CsSnI_3$-based inorganic perovskite solar cells based on a mesoscopic metal oxide framework via incorporating a donor element", *Journal of materials chemistry A*, v.

8, n. 12, pp. 4118–4124, 2020.

[138] CHUNG, I., SONG, J.H., IM, J., *et al.*, "$CsSnI_3$: Semiconductor or metal? High electrical conductivity and strong near-infrared photoluminescence from a single material. High hole mobility and phase-transitions", *Journal of the american chemical society*, v. 134, n. 20, pp. 8579–8587, 2012.

[139] BARANWAL, A.K., SAINI, S., WANG, Z., *et al.*, "Interface engineering using Y_2O_3 scaffold to enhance the thermoelectric performance of $CsSnI_3$ thin film", *Organic Electron*ics, v. 76, n. 9, pp. 105488, 2020.

[140] WANG, Y., TU, J., LI, T., *et al.*, "Convenient preparation of $CsSnI_3$ quantum dots, excellent stability, and the highest performance of lead-free inorganic perovskite solar cells so far", *Journal of materials chemistry A*, v. 7, n. 13, pp. 7683–7690, 2019.

[141] ZHU, P., CHEN, C., GU, S., *et al.*, "$CsSnI_3$ solar cells via an evaporation-assisted solution method", *Solar RRL*, v. 2 n. 4, pp. 1–5, 2018.

[142] SHAKIL, M., AKRAM, A., ZEBA, I., *et al.*, "Effect of mixed halide contents on structural, electronic, optical and elastic properties of $CsSnI_{3-x}Br_x$ for solar cell applications: First-principles study", *Materials res earch express.*, v. 7, n. 12, pp. 1-13, 2020.

[143] LI, W., LI, J., LI, J., *et al.*, "Addictive-assisted construction of all-inorganic $CsSnIBr_2$ mesoscopic perovskite solar cells with superior thermal stability up to 473 K", *Journal of materials chemistry A*, v. 4, n. 43, pp. 17104-17110, 2016.

[144] SABBA, D., MULMUDI, H.K., PRABHAKAR, R.R., *et al.*, "Impact of anionic Br^- substitution on open circuit voltage in lead free perovskite ($CsSnI_{3-x}Br_x$) solar cells", *The journal of physical chemistry C.*, v. 119, n. 4., pp. 1763–1767, 2015.

[145] HARTMANN, C., GUPTA, S., BENDIKOV, T., *et al.*, "Impact of SnF_2 addition on the chemical and electronic surface structure of $CsSnBr_3$", *ACS Applied materials & interfaces*, v. 12, n. 10, pp. 12353–12361, 2020.

ORCID

Cristian M. Díaz-Acosta https://orcid.org/0000-0002-9133-4684
Antonia Martínez-Luévanos https://orcid.org/0000-0003-3499-1693
Sofía Estrada-Flores https://orcid.org/0000-0003-4706-3984
Lucía F. Cano-Salazar https://orcid.org/0000-0003-2437-3728
Elsa N. Aguilera-González https://orcid.org/0000-0002-6289-5992
M. Cristina Ibarra-Alonso https://orcid.org/0000-0002-5719-8164